arXiv:0707.4435v2 [cond-mat.other] 12 Apr 2008

Emulating Non-Abelian Topological Matter in Cold Atom Optical Lattices

V. W. Scarola and S. Das Sarma
Condensed Matter Theory Center, Department of Physics,
University of Maryland, College Park, MD 20742

(Dated: April 12, 2008)

Certain proposed extended Bose-Hubbard models may exhibit topologically ordered ground states with excitations obeying non-Abelian braid statistics. A sufficient tuning of Hubbard parameters could yield excitation braiding rules allowing implementation of a universal set of topologically protected quantum gates. We discuss potential difficulties in realizing a model with a proposed non-Abelian topologically ordered ground state using optical lattices containing bosonic dipoles. Our direct implementation scheme does not realize the necessary anisotropic hopping, anisotropic interactions, and low temperatures.

PACS numbers: 03.75.Lm

I. INTRODUCTION

Topological matter is operationally defined[1] as a two-dimensional quantum many-body system with a non-trivial ground state degeneracy immune to weak local perturbations. The existence of an excitation gap separating the ground state from the low-lying excitations guarantees quantum immunity of the ground state degeneracy against local perturbations. Topological matter sustains, in general, two types of excitations. With type I (type II) topological order quasiparticles obey Abelian (non-Abelian) statistics. Physically braiding excitations in type I and type II topological matter modifies the many-body wavefunction by a phase and non-trivial matrix, respectively. Braiding non-Abelian quasiparticles may enable fault-tolerant topological quantum computation[1,2], reducing stringent quantum error correction procedures required of ordinary qubit-based quantum computation. We further classify type II topological order based on potential application in topological quantum computation. Braiding a small number of excitations in type IIa topologically ordered matter does not yield a universal set of quantum gates necessary for implementing all quantum codes. Braiding in type IIa matter must be supplemented by unprotected quantum gates in order to implement an arbitrary quantum code thereby offering a "partial" topological immunity to weak local noise. Braiding excitations in type IIb systems, in contrast, yields a universal set of quantum gates offering "full" topological immunity in implementing an arbitrary quantum code with braid operations. Models demonstrating type IIb topological order incorporate additional complexity to accommodate a universal set of gates in the excitation braid structure.

Although a great deal is known theoretically about topological matter in the effective field theory sense, the necessary conditions for the emergence of topological order and non-Abelian quasiparticle statistics in real materials are not entirely known. A current candidate of type IIa topological order is the so-called $\nu = 5/2$ fractional quantum Hall state occurring at mK temperatures in GaAs based high mobility two-dimensional electron systems subjected to a strong external magnetic field. However, no direct experimental evidence exists establishing the non-Abelian topological nature of the $\nu = 5/2$ fractional quantum Hall state[3] or any real material. Similarly, it is conjectured[4] that the fragile and rarely observed 12/5 fractional quantum Hall state may be type IIb with anyonic quasiparticles (the so-called "Fibbonacci anyons") suitable for universal quantum computation, but little is known about the nature of this very weak state. It is, however, well-accepted[5,6] that the quasiparticle excitations of the well-known fractional quantum Hall states (i.e. 1/3, 2/3, 2/5, 3/7, and so on) are type I.

Given the absence of any experimentally definitive topological system, much theoretical work has gone into effective theoretical lattice models which have topological many-body ground states. The most famous example of a type IIa topological lattice model in the quantum information context is Kitaev's toric code[2], a two-dimensional spin lattice model. Another such example, of interest to our work presented in this paper, is a Bose-Hubbard lattice model on a kagome lattice with extended and ring exchange interaction terms which has been proposed as a model carrying type IIb topological order[7,8]. One possible advantage of the topological lattice models is that, although these lattice models are highly contrived from the solid state physics perspective (and their applicability to real solid state materials is completely unknown), it is, in principle, possible to imagine emulating them on cold atom optical lattices similar to what has been already experimentally achieved in realizations of the on-site Bose-Hubbard model with bosonic optical lattices[9,10,11]. Motivated by the remarkable success of quantum analog simulation of solid state models[12] several recent theoretical proposals have been made to create[13,14] and manipulate[15] cold atom optical lattices emulating Kitaev spin models[2,16].

In this paper we theoretically identify key issues in optical lattice emulation of the extended Bose-Hubbard model originally considered as a quasi-realistic lattice model by Freedman *et al.*[7,8]. While Refs. 7 and 8 study this model independent of specific experiments, it is natural to ask if experiments can approximate such a model. We analyze a "direct" optical lattice emulation of the topological extended Bose-Hubbard model with dipoles. By "direct" we mean optical lattices formed from interfering standing wave lasers containing bosons with a dipolar interaction. Our direct scheme combines recent work including optical lattice experiments[17], proposals[18], and results showing Bose-Einstein condensation with dipolar atoms[19]. We find that our direct implementation scheme would be extremely difficult, if not impossible, even as a matter of principle because the combined parameter constraints on the hopping, various interaction terms, superexchange, temperature, single band restriction, and chemical potential required to reach the proposed topological regime are, for all practical purposes, mutually exclusive. Specifically, we find that: i) Our lattice setup significantly alters chemical potentials to yield prohibitively long hopping times between sites (See Fig. 2) ii) Band effects in our lattice setup, combined with the isotropic dipolar interaction, do not induce a sufficient anisotropy in the interaction (we require an order of magnitude relative anisotropy among next nearest lattice sites but we achieve 8% at best), iii) The realization of many-body superexchange in harmonic optical lattices presents stringent constraints on temperature, T (See Fig. 3).

The plan of the paper is as follows: In section II we review relevant aspects of the extended Bose-Hubbard model of Refs. 7 and 8. In section III we calculate the Hubbard parameters for a direct implementation of an extended Bose-Hubbard model with dipoles confined in a kagome optical lattice. We attempt to modify the lattice to tune Hubbard parameters. We find that our lattice "coloring" scheme does not yield an appropriate set of Hubbard parameters. In section IV we discuss practical issues in realizing low temperature superexchange with harmonic optical lattices. We find that weak (harmonic) site confinement places prohibitive constraints on the temperature. In section V we summarize difficulties we encountered in implementing the topological extended Bose-Hubbard model. We emphasize that our work here underscores difficulties with our direct implementation scheme using dipoles.

II. MODEL

We consider an optical lattice setup which approximates a single band Bose-Hubbard model. In Refs. 7 and 8 it was argued that bosons hopping in a 2D kagome lattice (see left panel of Fig. 1) can realize quantum topologically ordered ground states of type IIb, with Bose-Hubbard parameters tuned to specific values. The proposal presents the following model with an additional ring exchange term[7,8]:

$$
\begin{aligned}
H_{\mathrm{TB}} &= -\sum_i \mu_i n_i - \sum_{<i,j>} t_{i,j}\left(b_i^\dagger b_j + h.c.\right) \\
&+ \frac{U_0}{2}\sum_i n_i(n_i-1) + U_{\hexagon}\sum_{(i,j)\in\hexagon} n_i n_j \\
&+ \sum_{(i,j)\in\bowtie,\notin\hexagon} V_{i,j} n_i n_j . \qquad (1)
\end{aligned}
$$

The μ_i define site dependent chemical potentials and n_i is the number operator. The second term indicates bond-specific nearest neighbor hoppings with energy gain t_{ij}, where b_j annihilates a boson at the site j. U_0 represents an onsite interaction energy penalty assumed to be the largest energy scale in the single band limit. $U_{\hexagon}$ is an energy penalty between particles on a given hexagon and is tuned to be large thereby preventing double occupancy of hexagons. With one particle per hexagon and uniform hopping one finds a degenerate manifold of boson configurations that can be thought of as dimer configurations where each dimer lies along a line connecting the center of each hexagon. The degeneracy can be lifted by modifying hoppings or adding inter-hexagon interaction energy penalties (the last term in Eq. 1). The latter impose an energy cost (to be matched with superexchange interaction energies) between next-nearest neighbors lying along bow-ties not within the same hexagon. A proposed tuning of μ_i, $t_{i,j}$, $V_{i,j}$, and an additional multi-site ring exchange term (not discussed here) drive the system towards type IIb topological order[7,8]. In the same context a simpler set of conditions were proposed for realizing type I ground states (the $k=1$ topological phase realized with Eqs. 9-14 in Ref. 8). Some of these conditions

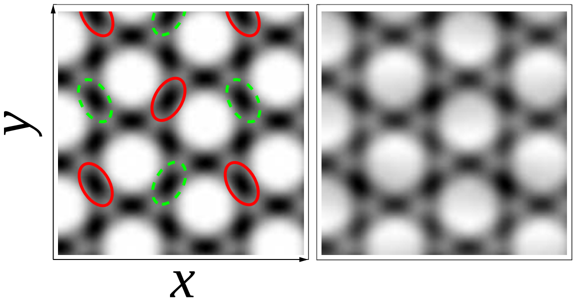

FIG. 1: Left panel: Grey scale plot of the kagome lattice, defined by Eq. 5, in the $x-y$ plane. Dark regions indicate sites. Sites encircled with solid (dashed) lines indicate red, r, (green, g,) sites. Sites not encircled indicate black, b, sites. Right panel: The same but with an additional potential (Eq. 6) added to color the lattice with $I_s = 0.3$.

are summarized below:

$$\begin{aligned}
\epsilon &= t^{\mathrm{b}}_{\mathrm{gb}}/U_{\hexagon} = t^{\mathrm{r}}_{\mathrm{bb}}/U_{\hexagon} \\
&= t^{\mathrm{b}}_{\mathrm{rb}}/(cU_{\hexagon}) \\
V^{b}_{gb}/U_{\hexagon} &= V^{b}_{bb}/U_{\hexagon} = 2ac\epsilon^2 \\
V^{b}_{rb}/U_{\hexagon} &= V^{b}_{rg}/U_{\hexagon} = 2c\epsilon^2/a \\
V^{r}_{bb}/U_{\hexagon} &= V^{g}_{bb}/U_{\hexagon} = 2\epsilon^2 \\
V_{i,j} &\ll U_{\hexagon} \\
t &\ll U_{\hexagon} \\
T &\ll t^2/U_{\hexagon} \\
\text{Interactions} &\ll \Delta. \qquad (2)
\end{aligned}$$

Here $t^{\gamma}_{\alpha\beta}$ indicates hopping between sites colored $\alpha \in$ {b,g,r} and $\beta \in$ {b,g,r} with $\gamma \in$ {b,g,r} the color of the site opposite α and β in the corresponding triangle, Fig 1. $V^{\gamma}_{\alpha\beta}$ indicates V_{ij} where α and β represent the colors of next-nearest neighbors i and j while γ is the color of the site between them. ϵ is a small positive number and c and a are constants. A modification of these conditions, involving additional complexity, may, as proposed in Refs. 7 and 8, drive the system towards type IIb topological order. The last two conditions depend on temperature and the energy splitting between the lowest and first excited band, Δ. They are practical constraints for a direct realization of a Hubbard model in a single band superexchange limit with low temperatures.

III. AN OPTICAL LATTICE OF DIPOLES

We now consider key difficulties in directly implementing the above tight binding model using bosons confined to optical lattices. Optical lattices offer a tunable environment free from defects, impurities, and lattice phonons. Implementations of Bose-Hubbard models have realized low temperature ($T \lesssim t$) superfluid and Mott phases[9,10,11]. These Bose-Hubbard systems have been realized with Alkali atoms parameterized by a zero-range contact interaction. Effectively contributing only U_0 in Eq. 1. Recent work seeks to extended the range of interaction between particles in optical lattices by promoting bosons to higher bands[20,21]. Promoting bosons to higher bands uses band effects to expand the contact interaction to include a weak nearest neighbor interaction. In implementing Eq. 1 we need interactions to be tuned over several nearest and next nearest neighbors. Work in a different system[19,22] highlights the possibility of confining dipoles to optical lattices. Dipoles in lattices generate nearest and next-nearest neighbor interaction terms in Hubbard models. Magnetic dipoles (e.g. ^{52}Cr) have a weak dipolar component (See, e.g., Ref. 23 for estimates). For example, lattice depths yielding a hopping of $0.1E_R$ leave a nearest neighbor interaction below $3\times10^{-4}E_R$ for $t \approx U_0$ with ^{52}Cr. But recent proposals indicate that molecules with electric dipolar moments may yield stronger dipolar contributions to the interaction (See, e.g., Refs. 18,24).

To be specific we assume that bosons with a strong dipolar interaction can be confined to optical lattices. The Hamiltonian for interacting particles of mass m in a single particle potential defined by an optical lattice, V_{OL}, is given by:

$$\begin{aligned}
H &= \sum_k \left[-\frac{\hbar^2}{2m}\boldsymbol{\nabla}^2_{\boldsymbol{r}_k} + V_{\mathrm{OL}}(\boldsymbol{r}_k) \right] \\
&+ \frac{1}{2}\sum_{k\neq l} V_{\mathrm{Int}}(|\boldsymbol{r}_k - \boldsymbol{r}_l|). \qquad (3)
\end{aligned}$$

To define a two-dimensional lattice in the $x-y$ plane we assume confinement along the z-direction, $V_z(z)$, sufficiently deep to prevent excitations out of the lowest confined state in the z direction. The z component of the wavefunction can be approximated by a Gaussian: $\phi(z) = (2/\pi l^2)^{1/4}\exp(-z^2/l^2)$, where l is defined by the confinement frequency along the z direction. The Fourier transform of the dipolar interaction (excluding the contact interaction), with the dipoles oriented along the z direction, is then[25]:

$$\tilde{V}^{2D}_{\mathrm{Int}}(\boldsymbol{k}_p) = g\left[\frac{1}{l\sqrt{\pi}} - \frac{3k_p}{2}\exp(l^2k_p^2)\mathrm{Erfc}(lk_p)\right], \quad (4)$$

where g is an interaction parameter, $\boldsymbol{k}_p = (k_x, k_y)$, and Erfc is the complimentary error function. In real space this interaction is isotropic, decays as r^{-3} at large distances, and has its short range part suppressed by the z extent of the wavefunction. We use the above interaction (including a contact interaction) to calculate the Hubbard parameters. We assume that the strength of the contact interaction and the dipolar interaction, g, are independently tunable over an arbitrary range.

The kagome lattice can be defined using six counter-propagating laser beams of wavevector k. By interfering the beams at specific angles the resulting potential is given by, $V_{\mathrm{OL}} = I_0 V_{\mathrm{kag}} + V_z$, where[18]:

$$\begin{aligned}
V_{\mathrm{kag}}(\boldsymbol{r}) &= \sum_{\alpha=1-3} [\cos(\boldsymbol{k}_\alpha\cdot\boldsymbol{r} + \phi_\alpha/2) \\
&+ 2\cos(\boldsymbol{k}_\alpha\cdot\boldsymbol{r}/3 + \phi_\alpha/6)]^2. \qquad (5)
\end{aligned}$$

With $\boldsymbol{k}_1 = k(-1/2, -\sqrt{3}/2), \boldsymbol{k}_2 = k(1/2, -\sqrt{3}/2), \boldsymbol{k}_3 = k(1,0), \phi_1 = -\phi_2 = \phi_3 = \pi$, and $I_0 = -E_{\mathrm{R}}/2$ the potential minima define an "isotropic" kagome lattice (see the left panel in Fig. 1). We define $E_{\mathrm{R}} = h^2/8ma^2$ with $a = \pi/k$. We use the tight binding basis of localized states (Wannier functions) centered at sites arranged in a kagome lattice. To calculate the Hubbard parameters we approximate the Wannier functions by Gaussians in a variational ansatz[18]. We minimize the single particle part of Eq. 3 with respect to four variational parameters, the Gaussian width and location, near each distinct site. For large lattice depths the Gaussian approximation provides a reasonable estimate of tight binding parameters calculated from a full band theory treatment[18].

The large number of interfering beams used to de the kagome lattice (Eq. 5) superpose to yield deep confine for $|I_0| \sim 0.5E_{\mathrm{R}}$. This is contrast to square o cal lattice geometries[9] that are safely in the single-ba tight-binding limit for much larger lattice depths (r $10E_{\mathrm{R}}$).

For dipoles in an isotropic kagome lattice defined V_{kag} the hopping, chemical potential, and interaction equal distances are all uniform throughout the latt Note that the spatial distance between site pairs ac a hexagon and along a bow-tie are the same. We fi by direct calculation, that the requirement $U_{\hexagon} \gg$ is therefore not satisfied by a kagome lattice of dip with a 2D spatially isotropic interaction. Furtherm the interaction between dipoles decays as r^{-3} leaving rections at large distances. We ignore corrections to interaction beyond the next-nearest neighbor. In pha with an energy gap ($\sim \mathcal{O}(\epsilon^2)$ in our example here) assume that the long range correction terms are much smaller than the gap thereby preventing a phase transition. This approximation depends on a theoretical unknown, the stability of the gapped topological phase with respect to perturbations. Emulating a topological phase in optical lattices would present us with an experimental tool to probe stability. We therefore ask if some of the conditions imposed on $V_{i,j}$ (Eqs. 2) can be partially met with the short range part of the dipolar interaction. Here we must match superexchange terms $\mathcal{O}(t^2/U_{\hexagon})$ with interaction terms, $V_{i,j}$.

We attempt to impose anisotropy in the lattice by tuning c in Eqs. 2 with a shifted potential. Applying an additional set of counter-propagating beams can, at least in principle, be used to "color" the otherwise uniform kagome lattice. Recent experiments have colored a two-dimensional square lattice[17]. We have here a dual goal: i) Can we color hoppings in accord with Eqs. 2? ii) Do band effects in the colored lattice induce substantial (order of magnitude) anisotropies in the interaction? We study an applied shift potential established by four additional beams to modify the hopping in an anisotropic fashion:

$$\begin{aligned} V_{\mathrm{s}}(\boldsymbol{r}) = &[\cos(\boldsymbol{k}_4 \cdot (\boldsymbol{r} - \boldsymbol{R}_1)) + A\cos(\boldsymbol{k}_5 \cdot (\boldsymbol{r} - \boldsymbol{R}_1))]^2 \\ &+ [\cos(\boldsymbol{k}_4 \cdot (\boldsymbol{r} - \boldsymbol{R}_2)) + A'\cos(\boldsymbol{k}_5 \cdot (\boldsymbol{r} - \boldsymbol{R}_2))]^2, \end{aligned} \quad (6)$$

where $\boldsymbol{k}_4 = k(1/3, 0), \boldsymbol{k}_5 = k(0, \sqrt{3}/6), \boldsymbol{R}_1 = a(-1/4, \sqrt{3}/4), \boldsymbol{R}_2 = a(-1/4, 5\sqrt{3}/4), A = 2.75$, and $A' = 1.9$. The first term in the potential modifies the hoppings by widening specific sites in the hexagon while the second term maintains a balance among hoppings at the opposite sides of a hexagon in the kagome lattice. As a result of the shift the site specific potentials become modified to $V_{\mathrm{OL}} = I_0[V_{\mathrm{kag}} + I_s V_{\mathrm{s}}] + V_z$ (see the right panel of Fig. 1). The top panel in Fig. 2 shows that the resulting hoppings go from uniform, at $I_s = 0$, to site-dependent, at finite I_s. The potential, at first glance, yields hoppings which approximate a tuning of c according to Eqs. 2. Note that $t_{3,4}$ is not in accord with Eqs. 2. The kagome lattice in Fig. 1 appears to be only slightly affected but this is in fact not the case. The bottom panel in Fig. 2 shows that the chemical potentials are drastically modified by V_{s}. The hopping times from site to site become prohibitively long with these large chemical potential shifts ($\sim E_{\mathrm{R}}$) indicating that weak modifications of the hoppings (30%) in this implementation of the kagome lattice lead to unwanted large shifts in the chemical potential. In fact another crucial requirement in implementing Eq. 1 is the ability to tune the chemical potential locally to maintain uniform renormalized chemical potentials throughout the lattice up to $\mathcal{O}(t^2/U_{\hexagon})$. We find that modifying hoppings with Eq. 6 leads to drastic and incompatible changes in chemical potentials.

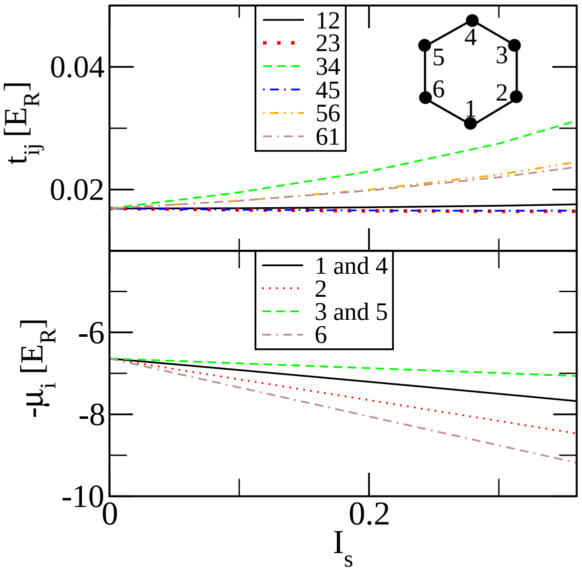

FIG. 2: Top panel: Hopping between site pairs around a hexagon as a function of the shift potential strength, I_s. The lower left hexagon from Fig. 1 is labeled $1-6$, where 2 is a green site. I_s approximately tunes c in Eqs. 2. Bottom panel: Chemical potential around the hexagon resulting from the addition of the shift potential to the kagome.

The lattice coloring scheme defined by V_{s} leads to anisotropic interactions. The colored lattice alters the shape of the Wannier functions in a site specific fashion and can therefore, in principle, induce anisotropies in the interaction. Eqs. 2 require that bow-tie terms, $V^{\gamma}_{\alpha\beta}$, are at least an order of magnitude smaller than hexagon terms, $U_{\hexagon}$. Since these interactions cover the same physical distance in the kagome lattice we require anisotropies in the interaction among next nearest neighbors. We find, by direct calculation, that band effects modify the next nearest neighbor interaction only slightly. There is, at best, a 8% anistropy in, e.g., the quantity $(V_{15} - V_{46})/V_{46}$, (See the site definitions in the top panel of Fig. 2) in the range $0 \leq I_s \leq 0.4$. The variation in bow-tie terms compared to cross-hexagon terms was much less, $< 1\%$, over the same range of I_s values.

IV. TOWARDS SUPEREXCHANGE

We now briefly discuss practical issues in realizing low temperature superexchange with particles in optical lattices modeled by Eq. 3. Nearly all proposed topological lattice models make use of a delicate competition between anisotropic interaction terms. Ref. 7 invokes superexchange to generate some of these interaction terms from an underlying Hubbard model. A variety of theoretical proposals in the optical lattice setting seek to realize the equivalent of superexchange with different techniques including the use of interstitials with resonant interactions[26] and polar molecules[14,27]. But, conventionally, superexchange in a single band Hubbard model can be achieved with low temperatures, $T \ll \mathcal{O}(t^2/U)$, and interaction strengths below the band gap, $U \ll \Delta$, where t and U are characteristic hopping and interaction energies, respectively. The temperature sets an absolute energy scale which can, in principle, be experimentally tuned below the superexchange limit, $\mathcal{O}(t^2/U)$. In practice, however, the realization of sufficiently low temperatures in optical lattice setups remains elusive and has been a motivating factor in recent theoretical work (See Refs. 14,26,27,28 for example). We find rather stringent requirements on temperatures needed to realize conventional low temperature/single band superexchange with our direct implementation scheme, because, as we will show below, single band and low temperature requirements are mutually exclusive.

One potential solution to the temperature problem is to simply increase energy scales. The physical energy scale, E_{R}, is fixed by the mass of the constituent particles and the wavelength of the lasers defining the optical lattice. We exclude the possibility of adjusting the mass and laser wavelength. With more tunable experimental parameters one can, however, increase t by lowering the lattice depth while increasing U_0 with, for example, a Feshbach resonance. But note that the temperature sets a lower bound for t while Δ sets an upper bound on interaction energies. Typically, t decreases exponentially with Δ for large lattice depths making the last two requirements in Eqs. 2 difficult to realize even with extremely low temperatures. To quantify the parameter window we consider one-dimensional examples below.

The precise functional form relating t and Δ depends on details of the single particle potential defining the lattice. In solid state systems lattice sites are typically defined by spatially local atomic cores. The resulting band gaps can be quite large even for large hopping strengths (band widths). For comparison, consider a one-dimensional Mathieu lattice[29] defined by interfering lasers. Expanding the potential near each site yields a parabolic (harmonic) confinement characteristic of optical lattices. (Note that the intensity profiles of standing wave laser beams will almost always yield a parabolic potential about each optical lattice site, as in Eq. 5) Consider the Kronig-Penney model[30] where, by contrast, individual sites are modeled by attractive delta function potentials. For well separated sites ($t \ll \Delta$) the band width in the Kronig-Penney model scales more favorably with band spacing:

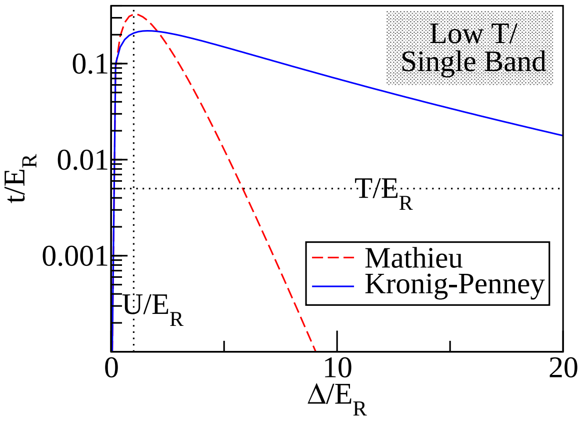

FIG. 3: Hopping versus band spacing for the one-dimensional Mathieu (dashed) and Kronig-Penney (solid) models, Eqs. 7. The vertical (horizontal) dotted line indicates an independently tunable interaction (temperature) scale. The upper right quadrant of the graph indicates a range of hoppings and band spacings that yield an ideal limit for superexchange given the positions of the dotted lines.

$$\begin{aligned} t_{\mathrm{M}}/E_{\mathrm{R}} &\approx \frac{4}{\sqrt{\pi}2^{3/4}}\left(\frac{\Delta}{E_{\mathrm{R}}}\right)^{3/2}\exp\left(-\sqrt{2}\Delta/E_{\mathrm{R}}\right) \\ t_{\mathrm{KP}}/E_{\mathrm{KP}} &\approx \left(\frac{\Delta}{E_{\mathrm{KP}}}\right)\exp\left(-\frac{\pi}{2}\sqrt{\Delta/E_{\mathrm{KP}}}\right), \end{aligned} \tag{7}$$

where $E_{\mathrm{KP}} = h/8ma_{\mathrm{KP}}^2$ for the Kronig-Penney model is defined in terms of a lattice spacing $a_{KP} = a$ to draw an equivalence with E_{R} for the optical lattice Mathieu problem. We derive Eqs. 7 under the assumption $t \ll \Delta$. The square root in the exponential suggests that Kronig-Penney-like systems (systems with tight confinement around each lattice site) are better approximated by single band models over a comparatively wider parameter range, provided equivalent energy scales. We show this in Fig. 3 where we plot Eqs. 7. The vertical and horizontal dotted lines indicate an arbitrarily tunable interaction energy and temperature, respectively. $T/E_{\mathrm{R}} = 0.005$ and $U/E_{\mathrm{R}} = 1$ are chosen as examples. The upper right quadrant of the graph then corresponds to the low temperature/single band limit ideal for realizing superexchange. The Kronig-Penney hopping and band spacing lead to a more favorable parameter window for superexchange. Harmonically confined sites (e.g. Eq. 5) require much lower temperatures.

V. CONCLUSION

We have discussed potential issues entering into our emulation scheme of a topological extended Bose-Hubbard model in cold atom optical lattices of dipoles finding that, even without considering the ring exchange terms in the proposed topological Hubbard model[7], it will be very difficult, if not impossible, to use our direct scheme to simulate the corresponding strongly correlated model of Ref. 7. We find: i) The constraint that the superexchange energy $\mathcal{O}(t^2/U_{\hexagon})$ is much larger than the temperature within the single-band Hubbard model (so that the band gap Δ is large compared with U_0 and $U_{\hexagon}$) is difficult to satisfy with currently accessible temperatures in experiments, $(T \sim t)$, using a direct emulation with harmonic optical lattices. This is currently a problem for most proposals making use of superexchange in optical lattices. A lattice with Kronig-Penney-like site confinement may allow a wider temperature window. Other implementation schemes[14,26,27,31], in conjunction with a kagome optical lattice[18], may also be able to avoid the prohibitively low temperature requirements. ii) Our suggested modifications to the kagome optical lattice, a tuning of hopping parameters with additional laser beams, lead to drastic and incompatible changes in the lattice structure itself. By tuning the lattice to color hoppings we find large chemical potential shifts ($\sim E_{\mathrm{R}}$) which correspond to prohibitively long hopping time scales. iii) We also find that, with dipoles, the constraints on the anisotropic interaction are too demanding for our direct implementation scheme. Specifically, cross-hexagon terms should be an order of magnitude larger than bow-tie terms, $V^{\gamma}_{\alpha\beta} \ll U_{\hexagon}$, but end up comparable in our scheme, $V^{\gamma}_{\alpha\beta} \sim U_{\hexagon}$. Tuning interaction anisotropy with band effects leads to only a small, $< 8\%$, variation in next nearest neighbor interaction terms. A low temperature optical lattice of polar molecules[31] may show more promise in all of the above categories. In spite of our somewhat disappointing conclusion on the prospects of creating a topological phase with an extended Bose-Hubbard model using kagome optical lattices, we think that it is important to continue thinking about cold atom optical lattices as suitable systems for emulating elusive type IIb topological phases by implementing other indirect techniques beyond the scope of our work. This is particularly true in view of the highly elusive nature of type IIb topological matter, and the fact that optical lattices allow for the possibility of emulating Hamiltonians which are unrealistic (certainly in their pristine forms) in solid state materials.

We thank J.I. Korsbakken, K. Park, K.B. Whaley, and C.W. Zhang for helpful discussions. This work is supported by the Microsoft Q Project and ARO-DARPA.

---

[1] S. Das Sarma, M. Freedman, C. Nayak, S. Simon, and A. Stern, arXiv:0707.1889.

[2] A. Kitaev, Annals Phys. **303**, 2 (2003).

[3] S. Das Sarma, M. Freedman, and C. Nayak, Phys. Rev. Lett. **94**, 166802 (2005).

[4] N. Read and E. Rezayi, Phys. Rev. B **59**, 8084, 1999.

[5] J.K. Jain, *Composite Fermions* (Cambridge University press, Cambridge, 2006).

[6] G.S Jeon, K.L. Graham, and J.K. Jain, Phys. Rev. B **70**, 125316 (2004).

[7] M. Freedman, C. Nayak, and K. Shtengel, Phys. Rev. Lett. **94**, 066401 (2005).

[8] M. Freedman, C. Nayak, and K. Shtengel, arXiv:cond-mat/0309120.

[9] D. Jaksch, C. Bruder, J. I. Cirac, C. W. Gardiner, and P. Zoller, Phys. Rev. Lett. **81**, 3108 (1998).

[10] M. Greiner, O. Mandel, T. Esslinger, T. W. Hansch, and I. Bloch, Nature (London) **415**, 39 (2002).

[11] I. Bloch, J. Dalibard, and W. Zwerger, arXiv:0704.3011.

[12] M. Lewenstein *et al.*, Adv. Phys. **55**, 243 (2007).

[13] L. M. Duan, E. Demler, and M. D. Lukin, Phys. Rev. Lett. **91**, 090402 (2003).

[14] A. Micheli, G. K. Brennen, and P. Zoller, Nature Physics, **2**, 341 (2006).

[15] C.W. Zhang, V.W. Scarola, S. Tewari, and S. Das Sarma, arXiv:quant-ph/0609101.

[16] A. Kitaev, Annals Phys. **321**, 2 (2006).

[17] J. Sebby-Strabley, M. Anderlini, P. S. Jessen, and J. V. Porto, Phys. Rev. A **73**, 033605 (2006).

[18] B. Damski *et al.*, Phys. Rev. Lett. **90**, 110401 (2003); B. Damski *et al.*, Phys. Rev. A **72**, 053612 (2005).

[19] A. Griesmaier, J. Werner, S. Hensler, J. Stuhler, and T. Pfau, Phys. Rev. Lett. **94**, 160401 (2005); T. Lahaye *et al.*, arXiv:0706.1670.

[20] V.W. Scarola and S. Das Sarma, Phys. Rev. Lett. **95**, 033003 (2005).

[21] T. Mueller, S. Foelling, A. Widera, and I. Bloch, arXiv:0704.2856.

[22] K. Goral, L. Santos, and M. Lewenstein, Phys. Rev. Lett. **88**, 170406 (2002).

[23] C. Menotti, M. Lewenstein, T. Lahaye, and T. Pfau, arXiv:0711.3422.

[24] L. Santos, G. V. Shlyapnikov, P. Zoller, and M. Lewenstein, Phys. Rev. Lett. **85**, 1791 (2000).

[25] P. Pedri and L. Santos, Phys. Rev. Lett. **95**, 200404 (2005).

[26] H.P. Buchler, M. Hermele, S. D. Huber, M. P. A. Fisher, and P. Zoller, Phys. Rev. Lett. **95**, 040402 (2005).

[27] H.P. Buchler *et al.*, Phys. Rev. Lett. **98**, 060404 (2007).

[28] S. Trebst, U. Schollwock, M. Troyer, and P. Zoller, Phys. Rev. Lett. **96**, 250402 (2006).

[29] J.C. Slater, Phys. Rev. **87**, 807 (1952).

[30] R. de L. Kronig and W. J. Penney, Proc. R. Soc. London Ser. A **130**, 499 (1930).

[31] J.I. Korsbakken and K. B. Whaley, private communication.